Attentional modulation of secondary somatosensory and visual thalamus of mice

Gordon H Petty[1] and Randy M Bruno[1,2,*]

[1] Department of Neuroscience, Columbia University, New York, NY 10027 USA

[2] Department of Physiology, Anatomy, & Genetics, University of Oxford, Oxford OX1 3PT, United Kingdom

* Correspondence: randy.bruno@dpag.ox.ac.uk (R.M.B.)

ABSTRACT

Each sensory modality has its own primary and secondary thalamic nuclei. While the primary thalamic nuclei are well understood to relay sensory information from the periphery to the cortex, the role of secondary sensory nuclei is elusive. One hypothesis has been that secondary nuclei may support feature-based attention. If this is true, one would also expect the activity in different nuclei to reflect the degree to which modalities are or are not behaviorally relevant in a task. We trained head-fixed mice to attend to one sensory modality while ignoring a second modality, namely to attend to touch and ignore vision, or vice versa. Arrays were used to record simultaneously from secondary somatosensory thalamus (POm) and secondary visual thalamus (LP). In mice trained to respond to tactile stimuli and ignore visual stimuli, POm was robustly activated by touch and largely unresponsive to visual stimuli. A different pattern was observed when mice were trained to respond to visual stimuli and ignore touch, with POm now more robustly activated during visual trials. This POm activity was not explained by differences in movements (i.e., whisking, licking, pupil dilation) resulting from the two tasks. Post hoc histological reconstruction of array tracks through POm revealed that subregions varied in their degree of plasticity. LP exhibited similar phenomena. We conclude that behavioral training reshapes activity in secondary thalamic nuclei. Secondary nuclei may respond to behaviorally relevant, reward-predicting stimuli regardless of stimulus modality.

INTRODUCTION

Each of the primary sensory cortices are reciprocally connected with corresponding sensory thalamic nuclei. These nuclei are broadly classified as primary or secondary (also known as high-order[1–3]). The primary nuclei respond robustly to sensory stimulation and transmit sensory information to the cortex[4–7]. By contrast, the secondary nuclei receive sparse input from the sensory periphery and are connected with many cortical and subcortical regions. They have nonspecific or complex receptive fields and their role in sensation and cognition is not well understood.

The rodent primary somatosensory cortex (S1) is connected to the posterior medial nucleus (POm), the secondary somatosensory thalamic nucleus[8,9]. Despite reciprocal connections with the whisker-sensitive region of S1, POm poorly encodes whisker touch and movement[10–12]. However, the region contributes to whisker-dependent behaviors[13,14], facilitates cortical plasticity[15–17], and encodes non-sensory task-related behaviors[18]. Despite these recent findings, POm activity in awake, behaving animals is relatively poorly understood.

There is evidence that the secondary nuclei also play a critical role in attention. The lateral posterior nucleus (LP) is the secondary visual thalamic nucleus in rodents, homologous to the lateral pulvinar in primates. In humans, damage to lateral pulvinar causes attentional deficits[19–21]. Similarly, pulvinar silencing in nonhuman primates induces transient impairment in attention tasks[22,23]. Secondary visual thalamus has not yet been similarly studied in rodents.

Despite belonging to ostensibly distinct sensory systems, there are several similarities in the activity and neuroanatomy between LP and POm: Both regions target primary and high-order sensory cortex in the same layer-specific way[7,18,24,25], have broad sensory receptive fields[11,25–27], and are driven by cortical activity rather than afferent sensory input[10,28–30]. These similarities suggest that the secondary nuclei could play similar roles in sensory processing and attention.

Here, we investigated how sensory-, arousal-, and movement-evoked activity in LP and POm are shaped by associative learning. We conditioned head-fixed mice to attend to a stimulus of one sensory modality (visual or tactile) and ignore a second stimulus of the other modality. We then recorded simultaneously from POm and LP. In mice trained to attend to a tactile stimulus and ignore a visual stimulus, tactile responses dominated throughout POm. In contrast, POm showed widespread visual responses in mice trained to respond to a visual stimulus and ignore touch. We observed similar effects in LP. Thus, behavioral training reshapes activity in secondary thalamus, inducing responses to behaviorally relevant stimuli regardless of sensory modality.

RESULTS

Mice can attend to one sensory modality while ignoring a second modality

We developed a conditioning task in which mice were trained to associate a stimulus of one sensory modality with a reward while ignoring a stimulus of a different modality. Water-restricted mice were head fixed and presented with a visual stimulus (a drifting grating on a monitor) and a tactile stimulus (an innocuous air puff to the distal ends of the whiskers) (Figure 1a). Mice were separated into two cohorts: in the “tactile” cohort a water reward was given at the offset of the air puff (Figures 1b, c top; n=11 mice); in the “visual” cohort the water reward was given at the offset of the drifting grating (bottom; n=12 mice).

Initially we trained mice on a shaping version of the task which followed a traditional trial-based structure (Figure 1b). A stimulus of one modality or the other was randomly presented on each trial. Trial-based structures are undesirable for our purposes because the unrewarded stimulus is informative that no reward will occur and may garner the animal's attention. Therefore, after reaching criterion (see Methods), mice were moved to the full version of the task. In the full task the stimuli were presented at the same mean rates as in the shaping task but were completely uncorrelated with one another (Figure 1c). After a stimulus, the time until the next stimulus of the same type was drawn from an exponential distribution plus a linear offset (Figure 1d, top). The *hazard rate* of the stimulus (the probability of the stimulus occurring at various times since the previous stimulus) was thus flat for the majority of possible inter-stimulus intervals (1d, bottom). Visual and tactile stimulus intervals were drawn independently, and the stimuli could overlap. As a result, given a stimulus, a mouse could not predict the timing of the next stimulus of either type. Naive mice trained on the full version of the task learned at a much slower rate than mice initially trained on the shaping version of the task and then advanced to the full task. We therefore trained all mice first on the shaping version of the task for at least three days and until they reached criterion before moving them to the full version (see Methods).

We examined anticipatory licking to assess how mice learned the stimulus-reward association (Figure 1e-j). For each stimulus presentation we computed a lick index (the difference in the number of licks during stimulus presentation and two seconds prior to stimulus onset, divided by the sum of all licks in both periods) [31]. A positive lick index indicates that a mouse responded to a stimulus by licking, a negative index indicates that it withheld licking, and an index of zero indicates that it ignored the stimulus.

An example visually conditioned mouse is presented in Figure 1e and f. During the shaping task, this mouse initially ignored both stimuli: the mouse did not lick in response to either the air puff or drifting grating, though it did lick to consume the water reward (Figure 1e, left). After several shaping sessions, the mouse learned that the drifting grating was predictive of a reward, as evidenced by an increase in licking after the onset of the drifting grating but before reward delivery (Figure 1e middle). However, this mouse also learned that the air puff predicted a *lack* of reward in the shaping task, as evidenced by withholding licking upon the onset of the air puff. The mouse thus displayed a positive visual lick index and a negative tactile lick index, suggesting that it attended to both the tactile and visual stimuli (Figure 1f, middle arrow).

In the full version of the task, the two stimuli are completely decorrelated, and the air puff is no longer predictive of the presence or absence of reward. After several sessions of conditioning on the full version of the task, the same mouse no longer altered its licking in response to the air puff (Figure 1e, right; Figure 1f, rightmost arrow). This indicates that the mouse learned to ignore the uninformative, distracting stimulus. All visually conditioned mice exhibited a similar learning trajectory (Figure 1i left, 1j left). These mice initially learned that the air puff indicated the absence of reward, sometimes before they responded to the visual stimulus at all. They only learned to ignore the air puff after several sessions of conditioning on the full version of the task.

By contrast, tactilely conditioned mice rapidly learned the association between air puff and reward, displaying a positive lick index as early as session 1 (Figure 1g, left; 1h). Tactilely conditioned mice always ignored the drifting grating, never displaying a visual lick index significantly different from zero (Figure 1i, right; figure 1j right). Such a discrepancy suggests that mice found this particular tactile stimulus more

113 salient than the drifting grating. In summary, mice can learn to disregard stimuli that lack information,
114 even when those stimuli are in and of themselves particularly salient.

115 *POm responses to tactile and visual stimuli depend on conditioning paradigm*

116 To evaluate the effect of reward conditioning on activity in secondary sensory thalamus, we performed
117 electrophysiological recordings in mice fully trained on the conditioning task (Figures 2 and 3). We inserted
118 a 64-channel multielectrode array that spanned both LP and POm. Probes were coated in DiI, and histology
119 images were aligned (see Methods) to identify the location of each putative cell (Figure 2a-c). Spike
120 clusters were manually curated based on waveform shape and spike autocorrelation (Methods, Figure S1a-
121 d). We identified 347 POm cells and 64 LP cells from 11 tactilely conditioned mice, and 257 POm cells and
122 67 cells from 12 visually conditioned mice. Our recordings covered most of the volume of POm but were
123 clustered primarily in the anterior and medial portions of LP (Figure 2d-f). Cells that were within 50 µm of
124 a region border were excluded from analysis. We observed no difference in waveform shape between POm
125 and LP, though POm cells tended to have a higher amplitude than LP cells (Figure S1e-i).

126 During recording, mice were presented with an equal number of air puffs and drifting gratings (80-120 of
127 each stimulus per mouse, median =100). We first investigated how conditioning affects POm activity. We
128 observed a heterogeneous population of cells with varied patterns of activity. For example, in tactilely
129 conditioned mice, we observed certain cells with a sharp increase in firing rate at air puff onset (Figure 3a,
130 left) and other cells that primarily responded after the stimulus offset when the mouse was consuming
131 the water reward (Figure 3a, right). A large portion of cells responded most strongly to the stimulus onset,
132 having a peak firing rate within 250 ms of the start of the air puff (70 cells, 20.2%). However, we also
133 observed cells with peak firing rates spanning the entire duration of the air puff and up to four seconds
134 after air puff offset (Figure 3c). Of cells from tactilely conditioned mice, 175 (50.4%) significantly responded
135 to the air puff, as defined by having a firing rate significantly different from baseline within one second
136 from air puff onset (Figure 3d, bottom). By contrast, only 24 cells (6.9%) had significant responses to the
137 drifting grating, and each of these cells also responded to the air puff (Figure 3d, top). No cells responded
138 to the drifting grating alone.

139 POm cells from visually conditioned mice exhibited a strikingly different pattern of activity (Figures 3b, e,
140 f). Surprisingly, many POm cells responded to the drifting grating alone or to both the drifting grating and
141 the air puff (Figure 3b, left). Others had no response to either stimulus but were more active during reward
142 consumption (Figure 3b, right). Compared to tactilely conditioned mice, a much larger portion of cells
143 responded to the onset of the drifting grating and a smaller portion responded to the air puff (Figure 3f,
144 16 air puff responding cells, 6.2%; 18 grating responding cells, 7%; 86 cells responding to both stimuli,
145 33.5%). Even when POm cells responded to both modalities, response latencies were lower for air puff
146 than drifting grating (Figure S2a, c). Further, POm visual responses often preceded a mouse's lick
147 responses. In summary, POm displayed dramatically different responses to visual and tactile stimuli
148 depending on the task type (Figure 3g).

149 In both conditioning groups, POm activity increased when mice were consuming water. We examined firing
150 rates during the offset period, defined as the two-second period after stimulus offset and during the
151 reward delivery (or absence of reward for the unconditioned stimulus). In both groups, cells had a greater

152 firing rate during the offset period (Figure 3h, Wilcoxon signed-rank test, $p<10^{-20}$ for both groups).
153 However, we did not observe a difference in activity between groups: air puffs in tactilely conditioned mice
154 and drifting gratings in visually conditioned mice were followed by similar amounts of POm activity
155 (p=0.82). This suggests that POm encoding of reward and/or licking is insensitive to task type, an
156 observation we examine further below.

157 *Modality selectivity varies with anatomical location in POm*

158 We considered the possibility that the differences in stimulus-aligned activity were caused by distinct
159 regions within POm having distinct sensory responses. We computed a selectivity index for each cell that
160 significantly responded to the air puff and/or the drifting grating (colored points in Figure 3d and 3f). A
161 selectivity index of +1 indicates that a cell responds only to the air puff, an index of -1 indicates that it
162 responds only to the drifting grating, and an index of 0 indicates that it responds to both stimuli with an
163 equal magnitude. Unresponsive cells (gray points in 3d and 3f) were excluded from this analysis.

164 All responsive cells in tactilely conditioned mice were tuned to touch (Figure 4a), and we found no pattern
165 between a cell's anatomical location and its selectivity index (Figure 4b, left). In visually conditioned mice,
166 POm neurons exhibited a wide variety of selectivity (Figure 4a). In these animals, touch selective cells
167 clustered in the lateral and dorsal region of POm (Figure 4b, right), a subregion receiving both top-down
168 inputs from the barrel cortex and ascending input from the brainstem[32,33]. Linear regression of selectivity
169 index against a cell's conditioning type and anatomical position along each axis (Figure 4c, see Methods)
170 revealed that only medial-lateral position was significantly correlated with selectivity index. Thus, there
171 appears to be a core location in the lateral most portion of POm that is always whisker sensitive, while
172 conditioning dictates the selectivity of the rest of POm.

173 *POm correlates with arousal and movement regardless of conditioning*

174 In freely-whisking mice, POm activity correlates with whisking, pupil radius, and behavioral state[11,12,34]. To
175 assess whether this correlation persists in our conditioning task and whether the conditioning type is a
176 factor, we acquired video of the whiskers and eye contralateral to the recorded thalamus (Figure 5a). We
177 measured pupil radius as a metric of arousal and quantified whisking activity by *amplitude*, the difference
178 between the most protracted and retracted position of the whiskers on each whisk cycle (Methods).
179 Whisking and pupil responses to stimuli were contingent on task type (Figure 5b). Tactilely conditioned
180 mice displayed a robust increase in pupil radius and whisking amplitude at the onset of the air puff (left).
181 This movement and arousal change persisted throughout the offset period. Tactilely conditioned mice did
182 not whisk in response to the drifting grating; however, the grating did induce a pupil constriction as
183 expected. We observed a similar pupil constriction at stimulus onset in visually conditioned mice, but this
184 was followed by pupil dilation (right). These mice also displayed increased pupil radius and whisking in
185 response to the unrewarded tactile stimulus, again suggesting that the whisker air puff is more salient than
186 the drifting grating even when a mouse has been trained to ignore it.

187 Consistent with previous results, we found that POm activity was correlated with both pupil and whisking
188 regardless of conditioning type (Figure 5c). Interestingly, POm neurons were more correlated with licking
189 after tactile conditioning than after visual conditioning. We have previously reported that POm correlates
190 with pupil radius most strongly at a time lag of about 1 second[34]. We found that visually conditioned POm

cells were more strongly correlated with pupil radius at this time lag compared tactile conditioning. However, this was not the case at a time lag of zero. This difference is likely due to the different pupil dynamics in response to the drifting grating across conditioning types.

Much of the stimulus-aligned POm activity observed could conceivably be due to movement and arousal responses rather than afferent sensory signals. To disentangle these, we fit the firing rate of each cell with a linear model using pupil radius, whisking amplitude, and lick rate as predictors on a trial-by-trial basis. We then analyzed the model residuals as a "movement-corrected" stimulus-evoked firing rate (Figure 5d, e). Compared to the raw firing rates (Figure 3g, h), we found that regressing out movement had little effect on activity during the stimulus period but resulted in reduced activity in the offset period. Thus, the apparent tactile and visual responses in POm after behavioral conditioning cannot be fully explained by movement or arousal.

Conditioning also reshapes LP activity

Conceivably, engaging in a visual or tactile task might differentially set the baseline activity of LP and POm accordingly. We first compared spontaneous firing rates, defined as the mean rate over periods that contained no licks, stimuli, or rewards for at least two seconds and that lasted at least 6 seconds. Conditioning type did not statistically change mean firing rates in POm or LP, though POm cells had a higher baseline firing rate on average (Figure 6a).

Like POm, LP exhibited a heterogeneous set of sensory responses that was highly dependent on conditioning (Figure 6b-d). In tactilely conditioned mice, the majority of LP cells responded to both the air puff and the drifting grating (23 cells, 36%) or the air puff alone (23 cells, 36%), with only 4 cells (6.3%) responding solely to the drifting grating. At the population level, LP firing rates during the air puff stimulus period were significantly higher than the drifting grating stimulus period (Figure 6e, left). In visually conditioned mice (Figure 6d) we observed far fewer cells responding only to the air puff (6 cells, 9%), but a similar proportion of cells that responded to the drifting grating or to both stimuli (8 grating responding cells, 11.9%; 27 cells responding to both stimuli, 40.3%). Similar to what we observed in POm, the magnitudes of air puff and grating responses were not significantly different (Figure 6e, right). Thus, tactile conditioning appears to potentiate tactile responses in LP. We did not observe a relationship between anatomical location and visual-tactile selectivity in LP (Figure S3); however, our recordings were concentrated on the anterior-medial portion of LP and thus may not characterize the entire nucleus.

As LP correlates with movement and arousal to the same degree POm does[34], we again computed a movement-corrected firing rate by regressing out pupil radius, whisking amplitude, and licking (Figure 6f). This regression quashed the difference in activity between conditioning types in the offset period only. Interestingly, we still observed an air puff response in visually conditioned LP even after this regression (Figure 6f, right). These results demonstrate that LP activity is similarly reshaped according to the modality of the attended stimulus.

DISCUSSION

Here, we investigated whether the secondary sensory thalamic nuclei differentially encode relevant and distracting stimuli. Our novel head-fixed conditioning paradigm demonstrates that mice can attend to a visual or tactile stimulus while ignoring a stimulus of the other sensory modality. The second modality neither enhanced nor suppressed action. Learning dramatically altered activity in POm: after visual conditioning, a large portion of POm cells responded to the onset of the visual stimulus. POm correlated with arousal and movement regardless of conditioning type, but movement correlations could not explain POm sensory responses. Learning also altered LP activity: LP responses to tactile stimuli were greater after tactile conditioning, while visual responses were weaker. The predominant response in both POm and LP was to the conditioned stimulus. Thus, the secondary sensory thalamic nuclei encode the behavioral relevance of a stimulus, regardless of its modality.

Learning is shaped by interactions of stimulus salience and behavioral relevance

We conditioned mice to lick in anticipation of a water reward after either a tactile stimulus (air puff) or visual stimulus (drifting grating). When trained on a traditional, trial-based structure, visually conditioned mice learned that the drifting grating predicted reward and that the air puff was negatively predictive of reward. Both stimuli modified action. In our novel design, however, the unrewarded stimulus was decoupled from reward entirely, making it a true distractor. When trained on this version of the task, visually conditioned mice learned to completely ignore the air puff. By contrast, tactilely conditioned mice always ignored the unrewarded drifting grating regardless of task structure. These mice also learned the stimulus-reward association after fewer sessions. The air puff was thus innately more salient than the drifting grating. Indeed, it is thought that mice rely more strongly on their whiskers than vision for many behaviors, and that all but the subtlest of vibrissa stimuli are salient[35]. Regardless, mice can be conditioned to completely ignore a salient stimulus in favor of a more behaviorally relevant one.

POm responds to behaviorally relevant stimuli regardless of modality

POm is only weakly activated by single whisker deflections, typically requiring large deflections of multiple whiskers to elicit a response[10,11,26]. These sensory responses likely arise from ascending input from somatosensory brainstem and/or descending input from primary somatosensory cortex[4,36,37]. Consistent with those studies, we observed POm cells that responded to the onset of the air puff in both conditioning groups. Tactilely conditioned mice exhibited many cells that responded not only to the onset of the air puff but also its entire seconds-long duration. Such responses were largely absent in visually conditioned mice.

Remarkably, we observed visual responses in POm after visual conditioning. These visual responses largely resembled the air puff responses in tactilely conditioned mice, with individual cells' activities tiling the entire duration of the stimulus. Visual responses in POm are unexpected. Though it receives excitatory input from a wide array of cortical regions[30,38,39], POm is not known to receive direct input from the retina or visual cortex. Rather than a sensory response *per se*, visual-evoked activity likely reflects encoding of behavioral state or attention. Consistent with that idea, many visually responsive cells also responded to the air puff. It could be that POm cells respond to any increase in attention, be it due to the unconditioned but salient, "attention grabbing" air puff or the subtler but now behaviorally relevant drifting grating.

There is growing evidence that POm is a heterogeneous region composed of multiple subnuclei defined by distinct thalamocortical outputs and corticothalamic inputs[18,32,33,40,41]. We found that the effects of

conditioning on POm sensory responses varied by anatomical location. While visual conditioning induced visual responses throughout POm, cells in the lateral dorsal region of POm remained more sensitive to the air puff than the drifting grating. Layer 5a cells in the S1 barrel field preferentially project to this region of POm[32], and POm cells receiving S1 corticothalamic input also receive convergent projections from the whisker-sensitive brainstem nucleus SpVi[32]. It is likely that the observed activity in lateral dorsal POm is driven by true whisker responses in SpVi and S1.

Movement does not explain POm plasticity

A recent study demonstrated that, in a tactile Go-NoGo paradigm, POm activity correlates with a mouse's decision to lick or withhold licking[18] and similar results have been demonstrated in a detection task using the forepaw[13]. Decision, response, and reward consumption coincide with movement – including whisking and licking. Responses in POm might instead be movement signals, though we have previously demonstrated that POm-whisking correlations cannot be fully explained by sensory reafference nor input from S1, M1, or the superior colliculus[34]. We found here that POm activity correlated with whisking amplitude, pupil diameter, and licking regardless of conditioning.

In both conditioning groups, POm activity was elevated during reward presentation and consumption, coincident with licking. POm receives somatotopic projections from all of S1, not just the barrel cortex[10,42]. As such, stimulation of the mouth and tongue - as occurs when the mouse licks - could contribute to POm activity via S1 during this period. Tactilely conditioned mice had a greater correlation between licking and POm activity. This could be a result of an increased sensitivity to all tactile stimulation as mice attend to the air puff, compared to mice that are ignoring the air puff and attending to the drifting grating.

Further, visually conditioned mice had a greater correlation between POm and pupil radius, but only at long time lags (>500 ms). Conceivably, as mice attend to visual stimuli, they could be more sensitive to all changes in retinal input, and this is reflected in POm activity. However, at time lags close to 0 ms there is no difference in POm-pupil correlation between tactile and visual conditioning groups, and we observe very few visually responsive cells in tactilely conditioned mice. Therefore, this activity may instead represent an increased correlation between POm and arousal. The drifting grating is inherently less salient than the air puff; consequently, the visual conditioning task may require greater attentional demands, which in turn could further engage the secondary thalamic nuclei.

As licking, whisking, and pupil dilation are all significantly correlated with POm, we examined whether this relationship could explain stimulus-evoked activity. Even after we factored out the possible contributions of these variables using regression, POm responses to the onset of conditioned stimuli were stronger than that of the unconditioned stimuli. In both tactilely and visually conditioned mice, movement could not explain the increased firing rate at air puff onset. These low-latency responses across conditioning groups is likely due in part to "true" sensory responses driven by S1 and SpVi. In tactilely conditioned mice, movement regression attenuated, but did not eliminate, activity in the later portion of the air puff. Activity in the rewarded offset period, however, was suppressed almost entirely, suggesting that post-stimulus activity is due to non-sensory signals when mice lick the water port.

LP activity is similarly shaped by conditioning

Like POm, LP displayed varied stimulus-evoked activity that was heavily dependent on conditioning. LP responded to the air puff robustly and with low latency, despite lacking direct somatosensory inputs. Though LP activity correlates with whisking and air puffs induce whisking, movement could not explain

such responses in either conditioning group. The air puff response was larger in tactilely conditioned mice, indicating that, like POm, LP is more responsive to the occurrence of any behaviorally relevant stimuli regardless of modality.

Unlike POm, LP responded to the drifting grating in both conditioning groups. LP receives input from the retina, the superior colliculus, and several visual cortical areas[25,28,29,43–45]. In tactilely conditioned mice, 42.3% of LP cells responded to the onset of the drifting grating, consistent with previous studies of LP responses to simple visual stimuli[27]. In visual conditioning animals, a greater portion of cells were visually responsive (52.2%), suggesting the existence of a population of LP cells that are not sensitive to simple visual stimuli but are active when a mouse is aroused and attentive.

LP has several sub regions with distinct cytoarchitecture, anatomical inputs, and retinotopic maps[24,28,29,46,47]. Our recordings were clustered in the anterior and medial portion of LP. These recording sites largely overlap with frontal LP, a region that receives input primarily from frontal cortex and only sparse input from V1 and superior colliculus. It is possible that the other regions of LP which receive greater input from visual cortex will be more responsive to visual stimuli and less affected by conditioning, similar to the dorsal-ventral region of POm we identified. Further characterization of the various LP subregions in behavioral contexts could reveal how specific cortical and subcortical inputs contribute to attention.

Possible mechanisms of non-sensory responses

What might be driving these non-sensory responses in the secondary nuclei? One likely mechanism is neuromodulation. Cortical levels of acetylcholine and norepinephrine track arousal[48]. Both acetylcholine and norepinephrine can act directly on thalamic nuclei like VPM[49,50] and may do so on POm and LP as well. Acetylcholine can also enhance POm tactile responses by suppressing GABAergic activity in the zona incerta[51]. LP receives inhibitory input from the zona incerta[52], so LP visual responses are likely modulated by cholinergic activity in the same way. Either direct modulation or indirect disinhibition could underlie enhanced air puff responses in tactilely conditioned POm and enhanced drifting grating responses in visually conditioned LP. State-based disinhibition of POm could also contribute to “visual” responses after visual conditioning by potentiating non-sensory inputs to POm.

Another potential culprit is direct corticothalamic input. S1 is thought to be the primary driver of POm[10]. Though S1 activity alone does not drive arousal-related activity in POm , direct S1-to-POm projections contribute to performance of tactile discrimination tasks[14]. Glutamatergic S1 inputs could underlie enhanced air puff responses in POm in behavioral contexts; however, S1 activity cannot explain the same effect in LP. Instead, visual responses in POm and tactile responses in LP might be driven by high-order cortex. In nonhuman primates, the lateral pulvinar has been shown to facilitate communication between the visual region V4 and higher order cortical regions. These include the lateral intraparietal area[53] and the temporo-occipital area[54], regions that are engaged in visual attention tasks. Indeed, there is growing evidence that the secondary nuclei may function as hubs for cortico-cortical communication[23,55,56]. Elevated activity in POm and LP could reflect increased cortico-cortical communication between high-order regions, primary sensory regions, and motor regions based on attentional needs.

The role of high-order thalamus in attention

The secondary visual thalamic nucleus in primates – the lateral pulvinar – has been known to play a role in guided visual attention. In humans, pulvinar damage causes a variety of attentional deficits, impairing

the ability to selectively attend to a visual stimulus in the presence of a distractor[20,21,21]. In nonhuman primates, chemical silencing of the pulvinar induces spatial neglect[22,23]. Further, pulvinar responses to a visual stimulus are strongest when a monkey directs attention towards that stimulus[57]. Similar results have not yet been reported in rodent LP, nor have they been directly extended to the somatosensory thalamus.

A consistent result of attention studies in humans and nonhuman primates is the enhancement of cortical and thalamic sensory responses to an attended visual stimuli.[23,58,59] Here, we show not just enhancement of sensory responses to stimuli within a single modality, but also across modalities. It is worth investigating further how secondary thalamus and high-order sensory cortex encode attention to stimuli outside of their respective modalities. Our surprising conclusion that the nuclei are equivalently activated by behaviorally relevant stimuli is nevertheless compatible with these previous studies.

The role of secondary thalamus in learning and cortical plasticity

Experience-dependent synaptic plasticity is a substrate of learning and memory. In anaesthetized mice, POm excitation facilitates long-term plasticity (LTP) in layer 2/3 pyramidal cells in S1, while POm silencing blocks plasticity[16]. Similarly, whisker-dependent associative learning potentiates POm-to-S1 synapses[15]. In visual cortex, excitation of layer 2/3 neurons paired with stimulation of layer 4 cells induces LTP in those layer 2/3 cells[60]. LP thus likely contributes to cortical plasticity. Elevated firing rates in POm and LP could contribute to learning the behavioral relevance of novel stimuli. That is, they may open a window of plasticity during periods of high arousal and task engagement. As such, we expect that disruption of thalamocortical output from secondary nuclei to sensory cortex (via optogenetic manipulation, *e.g.*) will disrupt or even prevent associative learning. Based on our findings, disruption of POm activity could impair even visual learning, and disruption of LP activity tactile learning, particularly if there were a strong multimodal component in the task. Such future experiments would further illuminate how the secondary nuclei participate in sensory processing and could pave the way for further studies of thalamocortical and corticothalamocortical circuits.

Conclusion

Our study demonstrates that a secondary sensory thalamic nucleus is dramatically modulated by behaviorally relevant events both in its modality as well as other modalities. This broad dependence on task engagement across secondary nuclei suggests a potential role in gating cortical plasticity and overall attention, particularly with regards to multimodal associative learning and transthalamic communication between cortical areas.

METHODS

Surgery

Mice were anaesthetized with isoflurane and placed in a stereotax. The scalp and fascia were removed, and a custom-cut stainless steel headplate was affixed with Metabond®. Mice were allowed to recover for seven days before water restriction and behavioral training. After behavioral training, mice were again anaesthetized and a ~200 µm-wide opening was cut on the left side of the skull, centered at 1.8 mm posterior to bregma and 1.5 mm lateral of the midline. The dura was removed to expose the surface of the brain. This craniotomy was then covered with Kwik-Cast™ silicone sealant. A silver wire or screw was inserted over the frontal cortex of the right hemisphere for use as a ground pin. Mice were then allowed to recover for 24 hours, after which the sealant was removed and recordings were performed. At the end of experiments, mice were deeply anesthetized with isoflurane and then perfused transcardially with phosphate buffer followed by 4% paraformaldehyde.

Behavior Apparatus

The behavior apparatus was contained in a black box with a light-blocking door. It was constructed from metal posts on an aluminum breadboard (Thorlabs). Mice were held in a 3D-printed hutch and head-fixed with a machined steel head plate holder. Air puffs (0.5-1 PSI) were delivered through a nozzle (cut p1000 pipet tip, approximately 3.5mm diameter aperture) and controlled by a solenoid. Water rewards (8-16µL) were similarly delivered by a solenoid. Licking was recorded with an infrared proximity detector. The visual stimulus was presented on a monitor (5 inch, 800x480 resolution, Eyoyo) positioned 11 cm from right side of the mouse hutch occupying 52°x 33° of visual space. The stimulus consisted of vertical drifting bars (Spatial frequency 0.05°/cycle, temporal frequency 1.5Hz) with maximum contrast (maximum luminance 247 cd/m^2, minimum luminance 3.2 cd/m^2). When the stimulus was off the monitor displayed a gray background set to the same mean luminance as the stimulus (125 cd/m^2). A photodiode was used to detect the onset of the visual stimulus to synchronize it with the rest of the apparatus.

An Arduino UNO microcontroller drove the two solenoids. A digital signal from the Arduino was used to trigger the visual stimulus, which was driven with a custom Python script (PsychoPy®). The solenoid TTL signals, the lick detector analog signal, and the photodiode output were all recorded with OpenEphys hardware and software (see “Electrophysiology” below). When capturing video, the Arduino also drove a blinking infrared LED to synchronize video data.

Conditioning

Mice were deprived of water 3 days prior to the start of conditioning. Throughout conditioning, mice were deprived of water in their home cages and received all daily water intake during the conditioning task. We closely monitored their weight and health, and *ad libitum* water was provided if weight decreased below 80% of baseline. Prior to conditioning, mice were habituated to head fixation and given *ad libitum* water in the behavior apparatus for 15-25 minutes.

In the first phase of conditioning (“shaping”), mice were separated into two cohorts: a “tactile” cohort and a “visual” cohort. Mice were presented with tactile stimuli (a two-second air puff delivered to the distal whisker field) and visual stimuli (vertical drifting grating on a monitor). Throughout conditioning, mice were monitored via webcam to ensure that the air puff only contacted the whiskers and did not disturb the facial fur nor cause the mouse to blink, flinch, or otherwise react – ensuring the stimulus was

innocuous. The stimulus types were randomly ordered. In the visual conditioning cohort, the visual stimulus was paired with a water reward (8-16µL) delivered at time of stimulus offset. In the tactile conditioning cohort, the reward was instead paired with the offset of the air puff. Regardless of the type of conditioning, stimulus type was a balanced 50:50 with an inter-stimulus interval of 8-12 seconds (uniform distribution). Mice were trained for one session per day, with each session consisting of an equal number of visual stimuli and air puffs. Sessions ranged from 20-60 minutes and about 40-120 of each stimulus.

Throughout training and during electrophysiology recordings, we recorded analog signals of mouth and tongue movements with an infrared proximity detector located below the water reward spout. Individual licks were detected by manually inspecting this signal and setting a threshold using custom MATLAB code. Throughout conditioning, we evaluated performance by measuring the anticipatory licking behavior of a mouse to a rewarded stimulus (CS+) or unrewarded stimulus (CS-). For each stimulus presentation, we counted the number of times a mouse licked in the two seconds prior to the stimulus onset and the number of licks during stimulus and calculated a lick index (LI) for that stimulus[31].

$$LI = \frac{licks_{stimulus} - licks_{baseline}}{licks_{stimulus} + licks_{baseline}}$$

A positive lick index indicates that a mouse responds to a stimulus by licking more and a negative index indicates that a mouse responds by withholding licking. Licks that occurred within 50 msec of the stimulus onset were excluded when computing the lick index.

Mice were trained on the shaping version of the task until the mean lick index of the CS+ for a given session was significantly greater than 0 (sign rank test), with a minimum of three days of conditioning. After reaching this threshold, mice were switched to the full version of the task. In the full task, the stimuli and reward were identical, but stimuli were presented at uncorrelated and less predictable intervals. For a given stimulus, the time until the next stimulus of the same type was drawn randomly from an exponential distribution with a mean of 10 seconds plus an offset of 8-12 seconds (draw from a uniform distribution), for a mean ISI of 20 msec. The maximum ISI was capped at 55 sec, and ISIs were binned by seconds. Both the air puff and the visual stimulus ISIs were drawn from the same distribution but were done so independently. Thus, the stimuli could overlap, the timing of the CS- was uncorrelated with the CS+ or the reward, and each stimulus had a largely flat hazard-rate for the majority of possible ISIs. Mice were then trained on the full version of the task until the mean LI per session for the CS- was not significantly different from 0, for a minimum of four days.

Electrophysiology

We performed simultaneous recordings from LP and POm from fully trained mice as the animal performed the full version of the task. Using a motorized micromanipulator (Scientifica PatchStar), we inserted a 64-channel electrode array (Cambridge Neurotech, models H3 and H9) into the craniotomy. Arrays were inserted vertically to a depth of 3.1-3.5 mm from the cortical surface (mean 3.4 mm). Prior to recording, the tip of the array was dipped into a DiI solution to label recording sites. Array recordings were acquired using an OpenEphys amplifier with two digital headstages (Intan RHD2132) at 30 kHz and with a bandwidth of 2.5 Hz to 7.6 kHz. The same acquisition system was used to record stimulus timing, licking, and a syncing signal for the video.

We used KiloSort3 to detect spikes and assign them to putative single units (Pachitariu et al., 2016) and Phy2 (https://github.com/cortex-lab/phy; Rossant, 2021) to manually inspect each unit. We merged units that appeared to originate from the same cell, based on waveform shape, auto- and cross-correlations, and firing rate over time. We excluded cells that lacked a refractory period (i.e. a dip in autocorrelation within 3ms). Specifically, units with more than 10% of spikes having inter-spike intervals shorter than 3msec were considered multi-unit and excluded. Units were assigned to the array channel on which its mean waveform was largest.

Histology

We sectioned paraformaldehyde-fixed brains into 100-µm sections using a vibratome. To visualize the border between POm and VPM, we stained sections for endogenous biotin using fluorescently conjugated streptavidin (Alexa Fluor 647, ThermoFischer). We imaged the sections on a slide scanner (Nikon AZ100 Multizoom). We then used SHARP-Track to align images to the Allen reference atlas and to identify the position of the electrode array by tracing the DiI track (Shamash et al 2018, https://github.com/cortex-lab/allenCCF). After histological alignment (see below) we used the depth of each putative cell along the array to assign it to a brain region. When assigning cells to brain regions, we excluded cells that were within 50 µm of a region boundary.

Videography

During electrophysiology recordings, two PS3 Eye cameras were used to capture video of the mouse's eye and whiskers. The whisker camera was positioned below the mouse's head and recorded at 125 fps. The eye camera was positioned on the right side of the face and recorded at 60 fps. The OpenEphys Bonsai program was used to record video.

Pupil size was measured from video offline using custom MATLAB code. We defined a region-of-interest around the eye and applied a threshold to each video frame to create a binary image of the pupil. We then used the function "regionprops" to fit an ellipse to the pupil and estimated pupil radius as the geometric mean of the semi-major and semi-minor axes of that ellipse. The trace of pupil radius over time was smoothed over 5 frames (8.3 msec). Large discontinuities in the pupil radius vector (such as those caused by a blink) were excluded based on a median filter (spanning 3 seconds) and linearly interpolated.

Whiskers were automatically tracked from videos using the software package *Trace* (Clack et al., 2012). Custom MATLAB software was used to compute the mean angle of all whiskers over each frame. The mean angle was bandpass filtered from 4 to 30 Hz and passed through a Hilbert transform to calculate phase. We defined the upper and lower envelopes of the unfiltered median whisking angle as the points in the whisk cycle where phase equaled 0 (most protracted) or $\pm\pi$ (most retracted), respectively. Whisking amplitude was defined as the difference between these two envelopes.

A blinking LED paired with a TTL pulse was used to synchronize the video frames to the data collected via the OpenEphys acquisition system. After processing the videos, this signal was used to align relevant video data (pupil radius and whisking amplitude, e.g.) to physiology and behavioral data. Video vectors were linearly interpolated from their respective frame rates to 1 kHz. Stimulus and licking signals were downsampled to 1 kHz, and spike times were rounded to the nearest millisecond.

Sensory Responses

We examined each cell's putative sensory response by comparing its firing rate during a "stimulus period" to its baseline firing rate. We first excluded overlapping stimuli, defined as any stimulus occurring within 6 seconds of a stimulus of a different type. We then counted the number of spikes that occurred within 1 second prior to the onset of each stimulus (baseline period) and within one second of the stimulus onset (stimulus period). The period within +/-50ms of the stimulus was considered ambiguous and excluded from analysis. We classified a cell's response as significant by first performing an ANOVA between all baseline firing rates and the rates during each stimulus period, followed by a Holm-Bonferroni multiple comparisons correction. This correction was applied to cells within each experimental group (*i.e.*, p values from tactile conditioning POm cells were corrected separately from p values of visual conditioning LP cells). We then classified cells as responding to the visual stimulus, the air puff, or both by performing paired Wilcoxon ranked-sum tests between stimulus period firing rates and the corresponding baseline firing rates. No multiple-comparisons correction was applied to the ranked-sum values.

For significantly responding cells, we computed a sensory response index (SI). Selectivity index measures the difference between the magnitudes of the air puff response and the drifting grating responses compared to the baseline firing rate.

$$SI = \frac{|FR_A - FR_B| - |FR_V - FR_B|}{|FR_A - FR_B| + |FR_V - FR_B|}$$

Where FR_B is the mean baseline firing rate, FR_A is the mean firing rate during the air puff stimulus period, and FR_V is the mean firing rate during the visual stimulus period. A positive selectivity index indicates that the cell has a larger response to an air puff, in terms of absolute change in firing rate, than it does to the visual stimulus, and vice-versa for a negative index.

To determine if anatomical location had a significant effect on sensory response index, we fit a linear model between the selectivity index of all POm cells and each cell's position in the dorsal-ventral (DV), medial-lateral (ML), and anterior-posterior (AP) position, along with the conditioning type (CT) of that cell. We also considered interactions between experiment type and position, but not between the different positional dimensions. The model thus had the following design:

$$SI \sim 1, DV, ML, AP, CT, CT * DV, CT * ML, CT * AP$$

To measure sensory response latency, we binned the firing rate of each cell into 10 ms bins. We measured the mean firing rate of each cell aligned to either the air puff or the visual stimulus. We then computed the mean and standard deviation of the cell's firing rate one second prior to the stimulus onset (baseline firing rate). We defined a sensory response as the first instance where a cell's activity increased or decreased to cross a 99% confidence interval (2.576 standard deviations) of the baseline firing rate for at least two consecutive time bins. Cells that did not meet this criterion within 500 ms of stimulus onset were excluded from further analysis of sensory response latency.

Regression of Movement and Arousal Variables

When fitting linear models, we first binned firing rates, lick rates, whisking, and pupil radius into 250-msec time bins. This bin size is long enough to capture a range of firing rates (i.e., most cells had multiple spikes per bin) while preserving the timing of licking and whisking. We tested models with bin sizes of 50, 100,

and 500 msec and found qualitatively similar results. For each cell, we fit a linear model of firing rate to whisking amplitude, pupil radius, and lick rate using least-squares regression. We extracted the model residuals for each cell, which correspond to a baseline-subtracted and movement-corrected firing rate.

ACKNOWLEDGMENTS

The authors thank Dahee Jang, Katy Willard, Candice Lee, Ziyue Liu, and Armin Lak for comments on the manuscript; Chris Rodgers and Sam Benezra for advice on creating the behavioral apparatus; and David Park for help training mice in pilot experiments. Support was provided by a Wellcome Trust Discovery Award, an Academy of Medical Sciences Professorship, NIH/NINDS R01 NS069679 and R01 NS094659, and NIH/NEI T32 EY013933.

FIGURE LEGENDS

Figure 1: Mice can be conditioned to attend to one sensory modality while ignoring a second modality.

a, Behavioral setup. Mice were head-fixed and presented with a visual stimulus (a drifting grating on a screen) or a tactile stimulus (an air puff to the distal portion of the whiskers). **b**, Schematic for the shaping version of the task, depicting the timing of the air puff (red), the drifting grating (dark blue), and the water reward (light blue). Mice were presented with either stimulus with an inter-stimulus-interval of 8-12 seconds. In the tactile cohort, the air puff was paired with a water reward; in the visual cohort the drifting grating was paired with the water reward. **c**, Schematic for the full version of the task. Stimuli were allowed to overlap so that only the conditioned stimulus predicted the timing of the water reward. **d**, Timing of stimuli in the full task. Inter-stimulus intervals were drawn from an exponential distribution with a linear offset (top). As a result, the hazard rate was largely flat for most stimulus presentations (bottom). **e**, Example behavior from a mouse trained on the visual task. Top row: raster plot of licks aligned to the onset of the grating (blue region). Red markers indicate the first lick to occur after reward was available. Middle row: raster plot of licks aligned to the onset of the air puff (red region). Bottom row: Mean lick rate aligned to the onset of the drifting grating (blue) or the air puff (red). Gray region indicates the stimulation period. Data are from the first session of the shaping task (left column), the first day of the full task (middle column), and the final day of conditioning (right column). **f**, Learning curve of the mouse shown in E, showing the lick index (mean +/- SEM) in response to the drifting grating (blue) or the air puff (red) on each training day. Vertical dotted line indicates the day the mouse was switched from the shaping version to the full version of conditioning. Triangles: sessions shown in e. **g, h**, Similar to e and f but for an example mouse trained on the tactile task. **i,** Learning curves of all visually conditioned mice (left) and tactilely conditioned mice (right). Thin lines: mean lick index of a single mouse. Thick lines: mean lick index across all mice. **j**, Mean lick index for all mice on the first day of conditioning ("shaping session 1"), the first day of the full task ("full session 1"), and the final conditioning session ("final full session").

Figure 2: Array recordings were made simultaneously from POm and LP.

a, Example coronal section. Red: DiI marking recording location. Gray: endogenous biotin stained with Alexa fluor 647 streptavidin. **b,** Zoom of the outlined region in a. The borders of LP, POm, and VPM are outlined. A 64-channel silicon probe was used to record from LP and POm. **c**, Mean waveform of an example POm cell across all probe channels. The channel with the largest mean waveform was identified and used to estimate the position of the cell (red circle in B). **d, e, f**, Estimated location of putative cells (gray circles) located in POm (red) and LP (blue) aligned to the Allen reference atlas. Cell locations are jittered along the medial-lateral and anterior-posterior axes for visualization purposes. **d**, Coronal projection over the range of cell locations in the anterior-posterior axis. **e**, Sagittal projection over range of cell locations in the medial-lateral axis. **f**, Transverse projection over range of cell locations in the dorsal-ventral axis.

Figure 3: POm responses to tactile and visual stimuli depend on conditioning paradigm.

a, Example cells from a tactilely conditioned mouse (same mouse as in figure 1e, conditioning session 7). Top row: spike raster aligned to the onset of the drifting grating (blue). Middle row: spike raster aligned to the air puff (red region). Bottom row: Mean firing rate over each trial aligned to the drifting grating (blue line) and the air puff (red line). Gray region indicates the timing of both stimuli. **b,** Sample cells from a visually conditioned mouse (same mouse as in figure 1c, conditioning session 12). **c**, Firing rate of all POm cells from tactilely conditioned mice aligned to either the air puff (left) or the drifting grating (right). Cells are sorted by the timing of the peak firing rate when aligned to the air puff. n=347 cells, 11 mice, range=11-57 cells/mouse, median=33 cells/mouse. **d**, Scatter plot of POm firing rates 1-second pre-stimulus (x-axis) and 1 second during stimulus onset (y-axis) from tactilely conditioned mice. Colored markers: cells with significantly different firing rates pre- and post-stimulus (1-way ANOVA with Holm-Bonferroni correction and post-hoc Wilcoxon signed-rank test). Gray markers: cells without significantly different firing rates. **e**, Firing rates of all POm cells from visually conditioned mice aligned to either the air puff (left) or the drifting grating (right). Cells are sorted by the timing of the peak firing rate aligned to the grating. (n=257 cells, 11 mice, range=10-42 cells/mouse, median=19 cells/mouse). **f**, Scatter plot of POm firing rates pre- and post-stimulus onset for visually conditioned mice, as in e. **g**, Event-triggered average firing rates of all POm cells (mean +/-SEM) aligned to either the air puff (red) or the drifting grating (blue) in tactilely conditioned mice (left) and visually conditioned mice (right). Gray region indicates the timing of both stimuli. **h**, Box plots of the change in firing rate from baseline for each POm cell during the first second of stimulus onset ("stimulus period") and during the first two seconds post-stimulus ("offset period"). In tactilely conditioned mice, firing rates were higher in the air puff offset period than the drifting grating offset period (two-way ANOVA with post-hoc Wilcoxon signed-rank test. Conditioning type F=2.06, p=0.15; stimulus type F= 138, p<0.001; interaction F=133, p<0.001; tactile conditioning Wilcoxon p<0.001; visual conditioning Wilcoxon p=0.58). In both conditioning types, firing rates in the offset period were significantly different between stimulus types (conditioning F=0.12, p=0.73; stimulus F=16, p<0.001; interaction F=304, p<0.001; Wilcoxon p<0.001 for both visually and tactilely conditioned mice).

Figure 4: POm responses to tactile and visual stimuli vary based on anatomical location.

a, Sensory response index for significantly responding POm cells (colored cells in 3d and 3f). Cells with a positive selectivity index primarily respond to the air puff and cells with a negative index primarily respond to the drifting grating. Cells from tactilely conditioned mice had a significantly higher response index (Wilcoxon rank sum test, p<0.001, n=200 tactile conditioning cells, 120 visual conditioning cells). **b**, Position of all POm cells separated by conditioning type. Cell positions are projected on the coronal plane (top row) and sagittal plane (bottom row), as in figure 2d and 2e. Significantly responding cells are colored by their response index. Gray Xs indicate nonresponding cells. Positions in the medial-lateral and anterior-posterior axes are jittered for visualization only. **c**, Response index of significantly responding cells as a function of their position in POm along the anterior-posterior (left), dorsal-ventral (middle), and medial-lateral axes (right). Light gray: tactile conditioning. Dark gray: visual conditioning. A linear model of response index with experiment type and anatomical position as predictors revealed a significant effect of medial-lateral position and an interaction between position and experiment type. In visually conditioned mice, cells in the lateral portion of POm were more selective to the air puff (model $p<10^{-60}$, adjusted $R^2=0.61$, conditioning $p<10^{-5}$, medial-lateral $p<10^{-4}$, ML-conditioning interaction $p<10^{-4}$, all other terms p>0.1)

Figure 5: POm correlates with arousal and movement regardless of conditioning.

a, Pupil and whisker tracking. Top left: Example frame from an eye video with the edge of the pupil highlighted in green. Top Right: A sample trace of pupil radius over time (gray: raw; green: smoothed). Bottom Left: Example frame from a whisker video with whiskers highlighted in green. Bottom Right: Example trace of whisker angle over time (gray) and the most protracted and retracted whisker positions over each whisk cycle (green), which is used to compute whisking amplitude. **b**, Whisking amplitude and pupil radius aligned to stimuli in tactilely conditioned mice (n=11 mice, left column) and visually conditioned mice (n=11 mice, right column). Top row: Pupil radius of each mouse aligned to either the air puff (blue) or the drifting grating (red) (Z-scored, mean+/-SEM). Bottom row: Whisking amplitude of each mouse aligned to the two stimuli (mean+/-SEM). Gray regions indicate stimulus timing. **c**, Cross-correlations between POm activity and pupil radius (top), whisking amplitude (middle), and lick rate (bottom). Light gray: Cells from tactilely conditioned mice (mean +/-SEM, n=347 cells, 11 mice). Dark gray: Cells from visually conditioned mice (n=257, 11 mice). Negative lags indicate that POm activity precedes the movement variable and positive lag indicates that POm activity follows the movement variable. **d**, Movement-corrected firing rates. The firing rate of each cell was fit to a linear model with whisking, licking, pupil radius, and baseline rate as predictors. Model residuals of all cells (mean+/-SEM) are aligned to the drifting grating and the air puff, as in B. **e**, Box plot of the model residuals of each POm cell during the first second of stimulus onset ("stimulus period"), and during the first two seconds post-stimulus ("offset period"), the same time windows as in 3g and 3h. Adjusted firing rates in tactilely conditioned mice were significantly higher during the air puff stimulus period than the drifting grating period. (Two-way ANOVA with post-hoc Wilcoxon signed-rank test. Conditioning type $F=4.23$, $p=0.04$; stimulus type $F= 68.2$, $p<0.001$; interaction $F=38.5$, $p<0.001$; tactile conditioning Wilcoxon $p<0.001$; visual conditioning Wilcoxon $p=0.09$). In visually conditioned mice, adjusted firing rates were higher during the drifting grating offset period than the air puff offset period. (conditioning $F=0.003$, $p=0.95$; stimulus $F=3.9$, $p=0.048$; interaction $F=9.45$, $p=0.002$; tactile conditioning Wilcoxon $p=0.94$, visual conditioning $p<0.001$).

Figure 6: Conditioning also reshapes LP activity.

a, Baseline firing rates of all POm and LP cells separated by conditioning type. POm cells had higher firing rates than LP cells, and firing rates did not significantly differ by conditioning type (two-way ANOVA, region $F=8.0$, $p=0.0049$; conditioning type $F=0.44$, $p=0.51$; interaction $F=1.44$, $p=0.23$). **b**, Example LP cells from a tactilely conditioned mouse (top) and a visually conditioned mouse (bottom). Mean firing rates over each trial are aligned to the drifting grating (blue line) and the air puff (red line). Gray region indicates the timing of both stimuli. **c**, Firing rate of all LP cells from tactilely conditioned mice aligned to either the air puff (left) or the drifting grating (right). Cells are sorted by the timing of the peak firing rate when aligned to the air puff. n=64 cells, 7 mice, range=4-16 cells/mouse, median=7 cells/mouse. **d**, Firing rate of all LP cells from visually conditioned mice aligned to either the air puff (left) or the drifting grating (right). Cells are sorted by the timing of the peak firing rate when aligned to the drifting grating. n=67 cells, 8 mice, range=1-19 cells/mouse, median=6 cells/mouse. **e**, Event-triggered average firing rates of all LP cells (mean +/SEM) aligned to either the air puff (red) or the drifting grating (blue) in tactilely conditioned mice (left) and visually conditioned mice (right). Gray region indicates the timing of both stimuli. **f**, Movement-corrected firing rates. The firing rate of each cell was fit to a linear model with whisking, licking, pupil radius, and baseline firing rate as predictors. Model residuals of all cells (mean+/-SEM) are aligned to the drifting grating and the air puff, as in E.

Figure S1: Manual curation of POm and LP cells

a, b, Example POm cells. *Left*, Mean spike waveform (black) with 200 randomly sampled individual waveforms (gray). *Right*, Autocorrelogram, binned at 0.5ms. Gray lines indicate a time lag of +/-1ms. **c, d**, Example LP cells, as in a and b. **e**¸ Mean waveforms of 50 randomly selected POm cells (red) and 50 randomly selected LP cells (blue). **f**, Histogram of waveform half-widths of each recorded POm cell (red, n=604) and LP cell (blue, n=131). **g**, Box chart of waveform half-width. Half-widths were not significantly different between LP and POm cells (POm: 0.40+/-0.07ms, LP: 0.41+/-0.08ms (mean+/-std), t-test p=0.052). **h**, Histogram of waveform amplitudes from each recorded POm and LP cell. **i**, Box chart of waveform amplitudes. POm cells had significantly higher amplitudes than LP cells (POm: 0.91+/-0.47mV, LP: 0.67+/-0.33mV (mean+/-std), t-test p<0.001).

Figure S2: Conditioning alters sensory response latency in POm and LP

a, b, Sample sensory response measurements of a POm cell from a visually conditioned mouse (a) and a LP cell from a tactilely conditioned mouse (b). A cell's response latency was measured as the first time the mean firing rate exceeded a 99% confidence interval for at least two 10 ms time bins. Red: firing rate aligned to air puff onset. Blue: firing rate aligned to drifting grating onset. Dotted gray line: 99% confidence interval of baseline firing rate. Black triangle: response latency. Cells that did not respond to a stimulus within 500 ms were excluded from further analysis. **c**, Box chart of POm response latency to the air puff after tactile conditioning (gray) and visual conditioning (white). The air puff response latency was shorter in visually conditioned mice (n=219 responding cells from tactilely conditioned mice, 130 from visually conditioned mice; p<0.005, Wilcoxon rank-sum test). **d**, LP response latency to the air puff. There was no difference in response latency to the air puff between tactilely and visually conditioned mice (n=57 responding cells from tactilely conditioned mice, 46 from visually conditioned mice; p=0.103). **e**, LP response latency to the drifting grating. Response latency was longer in visually conditioned mice (n=27 responding cells from tactilely conditioned mice, 25 from visually conditioned mice; p<0.001).

Figure S3: LP responses to tactile and visual stimuli as a function of anatomical location

a, Sensory response index for significantly responding LP cells. Cells with a positive selectivity index primarily respond to the air puff and cells with a negative index primarily respond to the drifting grating. Cells from tactilely conditioned mice had a significantly higher response index (Wilcoxon rank sum test, p<0.001, n=50 tactile conditioning cells, 41 visual conditioning cells). **b,** Position of all LP cells separated by conditioning type. Cell positions are projected on the coronal plane (top row) and sagittal plane (bottom row), as in figure 2d and 2e. Significantly responding cells are colored by their response index. Gray Xs indicate nonresponding cells. Positions in the medial-lateral and anterior-posterior axes are jittered for visualization only.

REFERENCES

1. Guillery, R.W., and Sherman, S.M. (2002). Thalamic Relay Functions and Their Role in Corticocortical Communication: Generalizations from the Visual System. Neuron *33*, 163–175. 10.1016/S0896-6273(01)00582-7.

2. Herkenham, M. (1980). Laminar organization of thalamic projections to the rat neocortex. Science *207*, 532–535. 10.1126/science.7352263.

3. Phillips, J.W., Schulmann, A., Hara, E., Winnubst, J., Liu, C., Valakh, V., Wang, L., Shields, B.C., Korff, W., Chandrashekar, J., et al. (2019). A repeated molecular architecture across thalamic pathways. Nature Neuroscience *22*, 1925–1935. 10.1038/s41593-019-0483-3.

4. Chiaia, N.L., Rhoades, R.W., Bennett-Clarke, C.A., Fish, S.E., and Killackey, H.P. (1991). Thalamic processing of vibrissal information in the rat. I. Afferent input to the medial ventral posterior and posterior nuclei. Journal of Comparative Neurology *314*, 201–216. 10.1002/cne.903140202.

5. Constantinople, C.M., and Bruno, R.M. (2013). Deep cortical layers are activated directly by thalamus. Science *340*, 1591–1594. 10.1126/science.1236425.

6. Sherman, S.M., and Guillery, R.W. (2002). The role of the thalamus in the flow of information to the cortex. Philosophical Transactions of the Royal Society of London. Series B: Biological Sciences *357*, 1695–1708. 10.1098/rstb.2002.1161.

7. Wimmer, V.C., Bruno, R.M., de Kock, C.P.J., Kuner, T., and Sakmann, B. (2010). Dimensions of a Projection Column and Architecture of VPM and POm Axons in Rat Vibrissal Cortex. Cerebral Cortex *20*, 2265–2276. 10.1093/cercor/bhq068.

8. Deschênes, M., Takatoh, J., Kurnikova, A., Moore, J.D., Demers, M., Elbaz, M., Furuta, T., Wang, F., and Kleinfeld, D. (2016). Inhibition, Not Excitation, Drives Rhythmic Whisking. Neuron *90*, 374–387. 10.1016/j.neuron.2016.03.007.

9. Petersen, C.C.H. (2007). The functional organization of the barrel cortex. Neuron *56*, 339–355. 10.1016/j.neuron.2007.09.017.

10. Diamond, M.E., Armstrong-James, M., Ebner, F.F., Armstrong-James, M., and Ebner, F.F. (1992). Somatic sensory responses in the rostral sector of the posterior group (POm) and in the ventral posterior medial nucleus (VPM) of the rat thalamus. Journal of Comparative Neurology *318*, 462–476. 10.1002/cne.903180410.

11. Moore, J.D., Mercer Lindsay, N., Deschênes, M., and Kleinfeld, D. (2015). Vibrissa Self-Motion and Touch Are Reliably Encoded along the Same Somatosensory Pathway from Brainstem through Thalamus. PLoS biology *13*, e1002253. 10.1371/journal.pbio.1002253.

12. Urbain, N., Salin, P.A., Libourel, P.A., Comte, J.C., Gentet, L.J., and Petersen, C.C.H. (2015). Whisking-Related Changes in Neuronal Firing and Membrane Potential Dynamics in the Somatosensory Thalamus of Awake Mice. Cell Reports *13*, 647–656. 10.1016/j.celrep.2015.09.029.

13. La Terra, D., Bjerre, A.-S., Rosier, M., Masuda, R., Ryan, T.J., and Palmer, L.M. (2022). The role of higher-order thalamus during learning and correct performance in goal-directed behavior. eLife *11*, 1–21. 10.7554/elife.77177.

14. Qi, J., Ye, C., Naskar, S., Inácio, A.R., and Lee, S. (2022). Posteromedial thalamic nucleus activity significantly contributes to perceptual discrimination. PLOS Biology *20*, e3001896. 10.1371/journal.pbio.3001896.

15. Audette, N.J., Bernhard, S.M., Ray, A., Stewart, L.T., and Barth, A.L. (2019). Rapid Plasticity of Higher-Order Thalamocortical Inputs during Sensory Learning. Neuron *103*, 277-291.e4. 10.1016/J.NEURON.2019.04.037.

16. Gambino, F., Pagès, S., Kehayas, V., Baptista, D., Tatti, R., Carleton, A., and Holtmaat, A. (2014). Sensory-evoked LTP driven by dendritic plateau potentials in vivo. Nature *515*, 116–119. 10.1038/nature13664.

17. Williams, L.E., and Holtmaat, A. (2019). Higher-Order Thalamocortical Inputs Gate Synaptic Long-Term Potentiation via Disinhibition. Neuron *101*, 91-102.e4. 10.1016/j.neuron.2018.10.049.

18. El-Boustani, S., Sermet, B.S., Foustoukos, G., Oram, T.B., Yizhar, O., and Petersen, C.C.H. (2020). Anatomically and functionally distinct thalamocortical inputs to primary and secondary mouse whisker somatosensory cortices. Nature Communications *11*, 1–12. 10.1038/s41467-020-17087-7.

19. Danziger, S., Ward, R., Owen, V., and Rafal, R. (2004). Contributions of the human pulvinar to linking vision and action. Cognitive, Affective, & Behavioral Neuroscience *4*, 89–99. 10.3758/CABN.4.1.89.

20. Snow, J.C., Allen, H.A., Rafal, R.D., and Humphreys, G.W. (2009). Impaired attentional selection following lesions to human pulvinar: evidence for homology between human and monkey. Proceedings of the National Academy of Sciences of the United States of America *106*, 4054–4059. 10.1073/pnas.0810086106.

21. Ward, R., Danziger, S., Owen, V., and Rafal, R. (2002). Deficits in spatial coding and feature binding following damage to spatiotopic maps in the human pulvinar. Nature Neuroscience. 10.1038/nn794.

22. Wilke, M., Turchi, J., Smith, K., Mishkin, M., and Leopold, D.A. (2010). Pulvinar inactivation disrupts selection of movement plans. The Journal of neuroscience : the official journal of the Society for Neuroscience *30*, 8650–8659. 10.1523/JNEUROSCI.0953-10.2010.

23. Zhou, H., Schafer, R.J., and Desimone, R. (2016). Pulvinar-Cortex Interactions in Vision and Attention. Neuron *89*, 209–220. 10.1016/j.neuron.2015.11.034.

24. Nakamura, H., Hioki, H., Furuta, T., and Kaneko, T. (2015). Different cortical projections from three subdivisions of the rat lateral posterior thalamic nucleus: A single-neuron tracing study with viral vectors. European Journal of Neuroscience *41*, 1294–1310. 10.1111/ejn.12882.

25. Roth, M.M., Dahmen, J.C., Muir, D.R., Imhof, F., Martini, F.J., and Hofer, S.B. (2016). Thalamic nuclei convey diverse contextual information to layer 1 of visual cortex. Nature Neuroscience *19*, 299–307. 10.1038/nn.4197.

26. Ahissar, E., Sosnik, R., and Haidarliu, S. (2000). Transformation from temporal to rate coding in a somatosensory thalamocortical pathway. Nature *406*, 302–306. 10.1038/35018568.

27. Allen, A.E., Procyk, C.A., Howarth, M., Walmsley, L., and Brown, T.M. (2016). Visual input to the mouse lateral posterior and posterior thalamic nuclei: photoreceptive origins and retinotopic order. The Journal of Physiology *594*, 1911–1929. 10.1113/JP271707.

28. Bennett, C., Gale, S.D., Garrett, M.E., Newton, M.L., Callaway, E.M., Murphy, G.J., and Olsen, S.R. (2019). Higher-Order Thalamic Circuits Channel Parallel Streams of Visual Information in Mice. Neuron *102*, 477-492.e5. 10.1016/j.neuron.2019.02.010.

29. Leow, Y.N., Zhou, B., Sullivan, H.A., Barlowe, A.R., Wickersham, I.R., and Sur, M. (2022). Brain-wide mapping of inputs to the mouse lateral posterior (LP/Pulvinar) thalamus–anterior cingulate cortex network. J Comp Neurol *530*, 1992–2013. 10.1002/cne.25317.

30. Liao, C.-C., Chen, R.-F., Lai, W.-S., Lin, R.C.S., and Yen, C.-T. (2010). Distribution of large terminal inputs from the primary and secondary somatosensory cortices to the dorsal thalamus in the rodent. Journal of Comparative Neurology *518*, 2592–2611. 10.1002/cne.22354.

31. Jurjut, O., Georgieva, P., Busse, L., and Katzner, S. (2017). Learning enhances sensory processing in mouse V1 before improving behavior. Journal of Neuroscience *37*, 6460–6474. 10.1523/JNEUROSCI.3485-16.2017.

32. Sumser, A., Mease, R.A., Sakmann, B., and Groh, A. (2017). Organization and somatotopy of corticothalamic projections from L5B in mouse barrel cortex. Proceedings of the National Academy of Sciences *114*, 8853–8858. 10.1073/PNAS.1704302114.

33. Groh, A., Bokor, H., Mease, R.A., Plattner, V.M., Hangya, B., Stroh, A., Deschenes, M., and Acsády, L. (2014). Convergence of Cortical and Sensory Driver Inputs on Single Thalamocortical Cells. Cerebral Cortex *24*, 3167–3179. 10.1093/cercor/bht173.

34. Petty, G.H., Kinnischtzke, A.K., Hong, Y.K., and Bruno, R.M. (2021). Effects of arousal and movement on secondary somatosensory and visual thalamus. eLife *10*, e67611. 10.7554/eLife.67611.

35. Warren, R.A., Zhang, Q., Hoffman, J.R., Li, E.Y., Hong, Y.K., Bruno, R.M., and Sawtell, N.B. (2021). A rapid whisker-based decision underlying skilled locomotion in mice. eLife *10*, e63596. 10.7554/eLife.63596.

36. Deschênes, M., Veinante, P., and Zhang, Z.-W. (1998). The organization of corticothalamic projections: reciprocity versus parity. Brain Research Reviews *28*, 286–308. 10.1016/S0165-0173(98)00017-4.

37. Veinante, P., Jacquin, M.F., and Deschênes, M. (2000). Thalamic projections from the whisker-sensitive regions of the spinal trigeminal complex in the rat. Journal of Comparative Neurology *420*, 233–243. 10.1002/(SICI)1096-9861(20000501)420:2<233::AID-CNE6>3.0.CO;2-T.

38. Aldes, L.D. (1988). Thalamic connectivity of rat somatic motor cortex. Brain Research Bulletin *20*, 333–348. 10.1016/0361-9230(88)90063-9.

39. Gharaei, S., Honnuraiah, S., Arabzadeh, E., and Stuart, G.J. (2020). Superior colliculus modulates cortical coding of somatosensory information. Nature communications *11*, 1693. 10.1038/s41467-020-15443-1.

40. Mease, R.A., Metz, M., and Groh, A. (2016). Cortical Sensory Responses Are Enhanced by the Higher-Order Thalamus. Cell Reports *14*, 208–215. 10.1016/j.celrep.2015.12.026.

41. Viaene, A.N., Petrof, I., and Sherman, S.M. (2011). Properties of the thalamic projection from the posterior medial nucleus to primary and secondary somatosensory cortices in the mouse. Proceedings of the National Academy of Sciences *108*, 18156–18161. 10.1073/pnas.1114828108.

42. Fabri, M., and Burton, H. (1991). Topography of connections between primary somatosensory cortex and posterior complex in rat: a multiple fluorescent tracer study. Brain Research *538*, 351–357. 10.1016/0006-8993(91)90455-5.

43. Born, G., Schneider-Soupiadis, F.A., Erisken, S., Vaiceliunaite, A., Lao, C.L., Mobarhan, M.H., Spacek, M.A., Einevoll, G.T., and Busse, L. (2021). Corticothalamic feedback sculpts visual spatial integration in mouse thalamus. Nat Neurosci *24*, 1711–1720. 10.1038/s41593-021-00943-0.

44. Juavinett, A.L., Kim, E.J., Collins, H.C., and Callaway, E.M. (2020). A systematic topographical relationship between mouse lateral posterior thalamic neurons and their visual cortical projection targets. Journal of Comparative Neurology *528*, 99–111. 10.1002/cne.24737.

45. Scholl, L.R., Foik, A.T., and Lyon, D.C. (2021). Projections between visual cortex and pulvinar in the rat. J Comp Neurol *529*, 129–140. 10.1002/cne.24937.

46. Takahashi, T. (1985). The organization of the lateral thalamus of the hooded rat. J Comp Neurol *231*, 281–309. 10.1002/cne.902310302.

47. Zhou, N.A., Maire, P.S., Masterson, S.P., and Bickford, M.E. (2017). The mouse pulvinar nucleus: Organization of the tectorecipient zones. Vis Neurosci *34*, E011. 10.1017/S0952523817000050.

48. Reimer, J., McGinley, M.J., Liu, Y., Rodenkirch, C., Wang, Q., McCormick, D.A., and Tolias, A.S. (2016). Pupil fluctuations track rapid changes in adrenergic and cholinergic activity in cortex. Nat Commun *7*, 13289. 10.1038/ncomms13289.

49. Aguilar, J.R., and Castro-Alamancos, M.A. (2005). Spatiotemporal Gating of Sensory Inputs in Thalamus during Quiescent and Activated States. 10.1523/JNEUROSCI.3229-05.2005.

50. Hirata, A., and Castro-Alamancos, M.A. (2010). Neocortex Network Activation and Deactivation States Controlled by the Thalamus. J Neurophysiol *103*, 1147–1157. 10.1152/jn.00955.2009.

51. Masri, R., Trageser, J.C., Bezdudnaya, T., Li, Y., and Keller, A. (2006). Cholinergic regulation of the posterior medial thalamic nucleus. Journal of Neurophysiology *96*, 2265–2273. 10.1152/jn.00476.2006.

52. Barthó, P., Freund, T.F., and Acsády, L. (2002). Selective GABAergic innervation of thalamic nuclei from zona incerta. European Journal of Neuroscience *16*, 999–1014. 10.1046/j.1460-9568.2002.02157.x.

53. Eradath, M.K., Pinsk, M.A., and Kastner, S. (2021). A causal role for the pulvinar in coordinating task-independent cortico–cortical interactions. Journal of Comparative Neurology *529*, 3772–3784. 10.1002/cne.25193.

54. Saalmann, Y.B., Pinsk, M.A., Wang, L., Li, X., and Kastner, S. (2012). The pulvinar regulates information transmission between cortical areas based on attention demands. Science (New York, N.Y.) *337*, 753–756. 10.1126/science.1223082.

55. Lohse, M., Cooper, M., Sader, E., Langfelder, A., Kahn, M., Baxter, L., Bartram, J., Phillips, J.W., Upton, A.L., and Mann, E.O. (2018). Motor cortex can modulate somatosensory processing via cortico-thalamo-cortical pathway. 366567. 10.1101/366567.

56. Theyel, B.B., Llano, D.A., and Sherman, S.M. (2010). The corticothalamocortical circuit drives higher-order cortex in the mouse. Nat Neurosci *13*, 84–88. 10.1038/nn.2449.

57. Petersen, S.E., Robinson, D.L., and Keys, W. (1985). Pulvinar nuclei of the behaving rhesus monkey: visual responses and their modulation. Journal of neurophysiology *54*, 867–886. 10.1152/jn.1985.54.4.867.

58. Gregoriou, G.G., Gotts, S.J., Zhou, H., and Desimone, R. (2009). High-Frequency, long-range coupling between prefrontal and visual cortex during attention. Science *324*, 1207–1210. 10.1126/science.1171402.

59. Moran, J., and Desimone, R. (1985). Selective attention gates visual processing in the extrastriate cortex. Science (New York, N.Y.) *229*, 782–784. 10.1126/science.4023713.

60. Kirkwood, A., and Bear, M.F. (1994). Hebbian synapses in visual cortex. J. Neurosci. *14*, 1634–1645. 10.1523/JNEUROSCI.14-03-01634.1994.

Figure 1: Mice can be conditioned to attend to one sensory modality while ignoring a second modality.

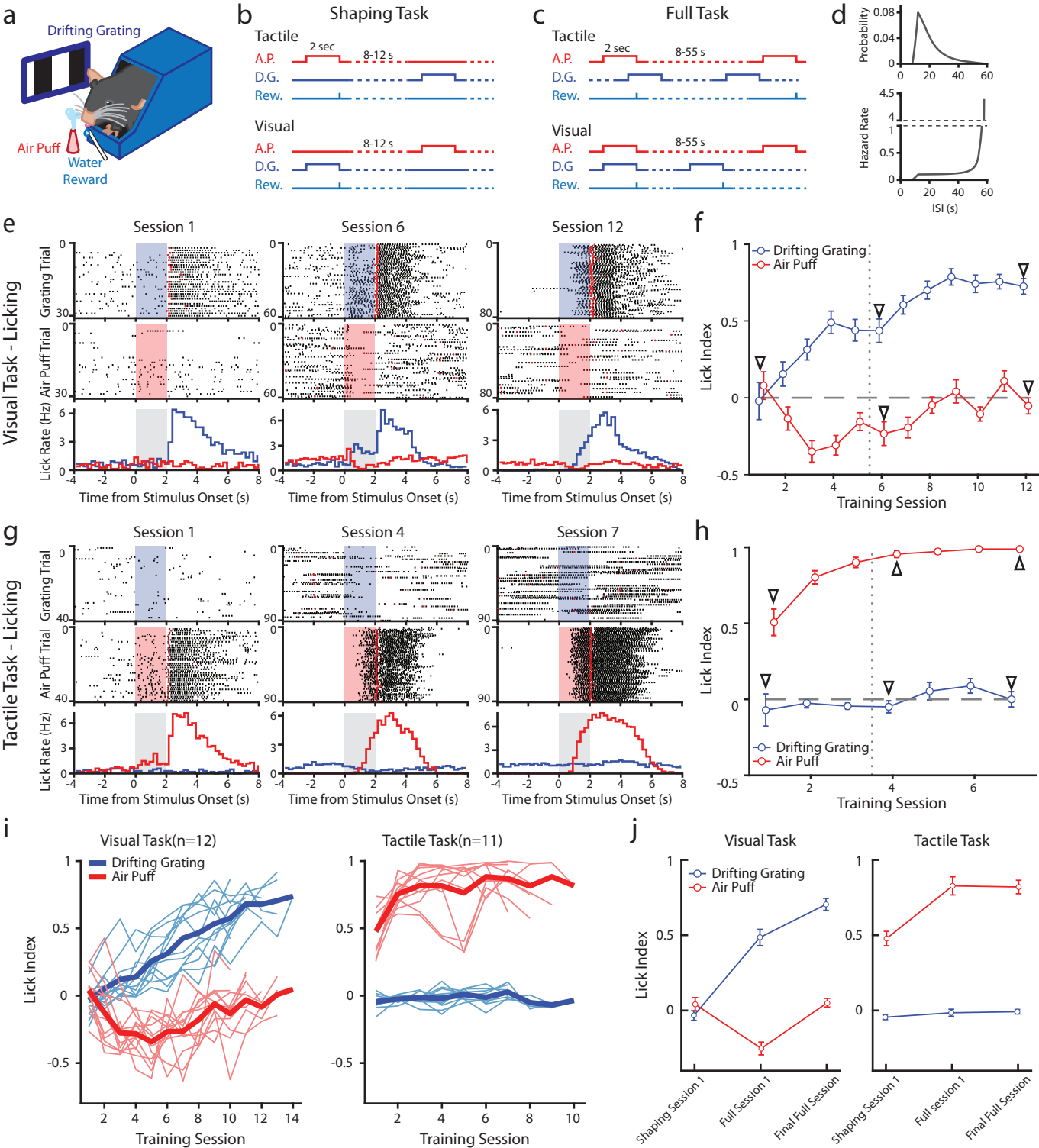

Figure 2: Array recordings were made simultaneously from POm and LP

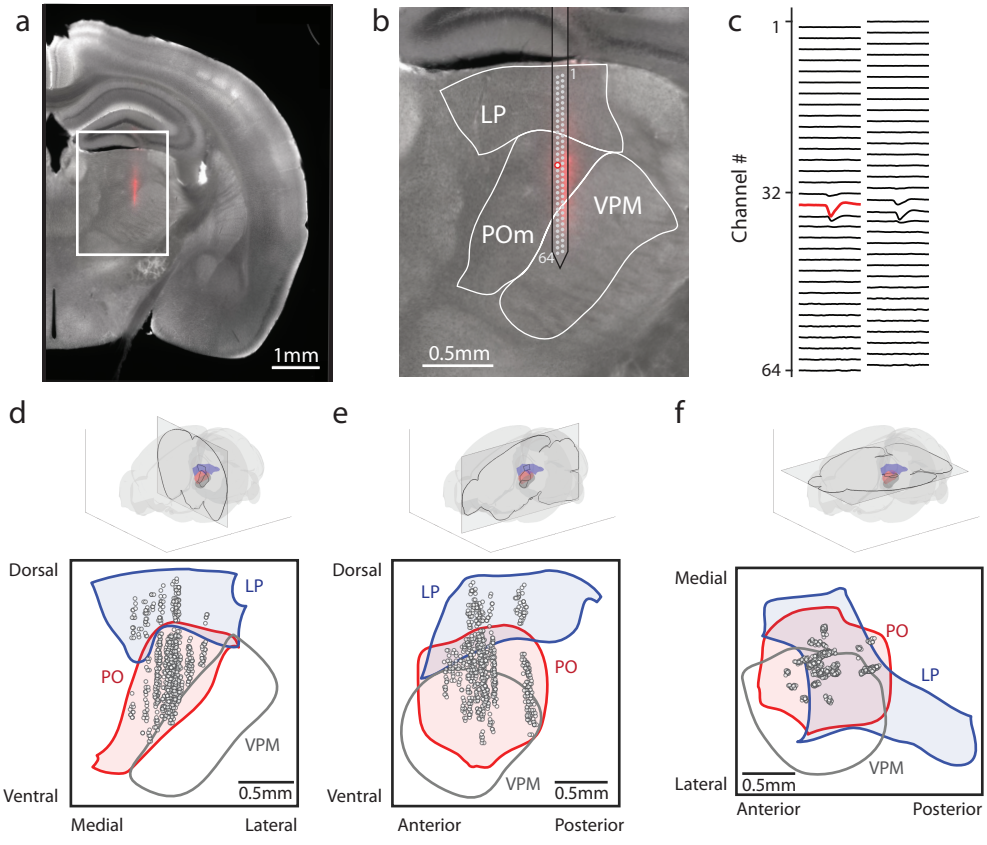

Figure 3: POm responses to tactile and visual stimuli depend on conditioning paradigm

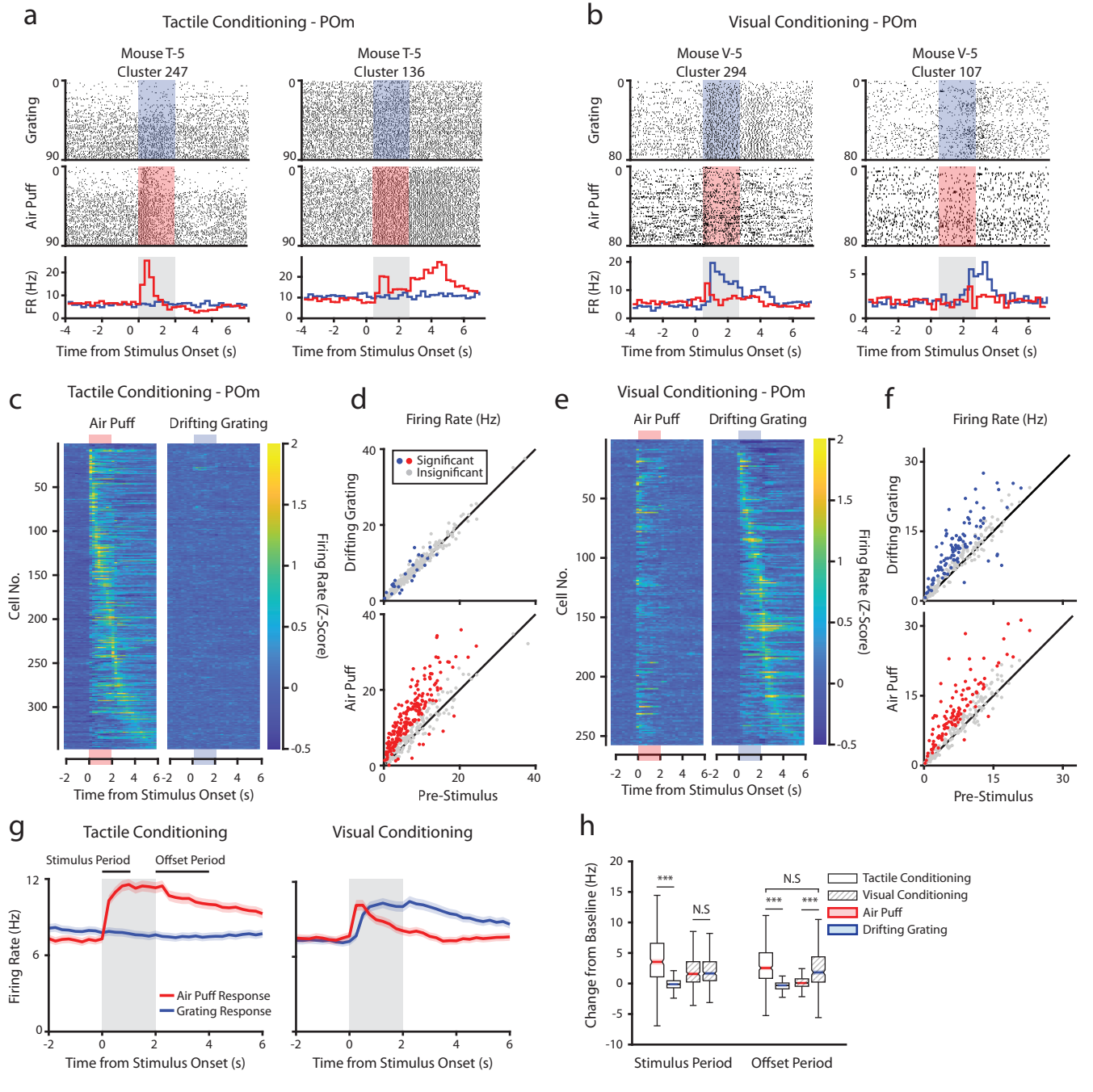

Figure 4: POm responses to tactile and visual stimuli vary based on anatomical location.

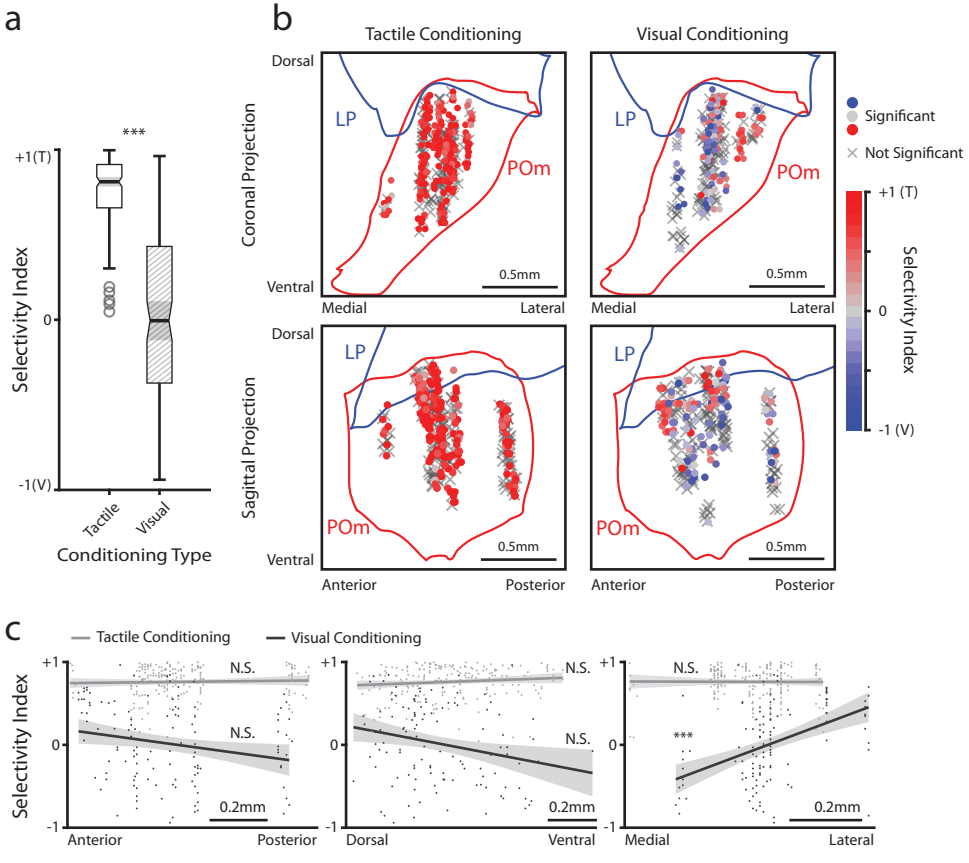

Figure 5: POm correlates with arousal and movement regardless of conditioning.

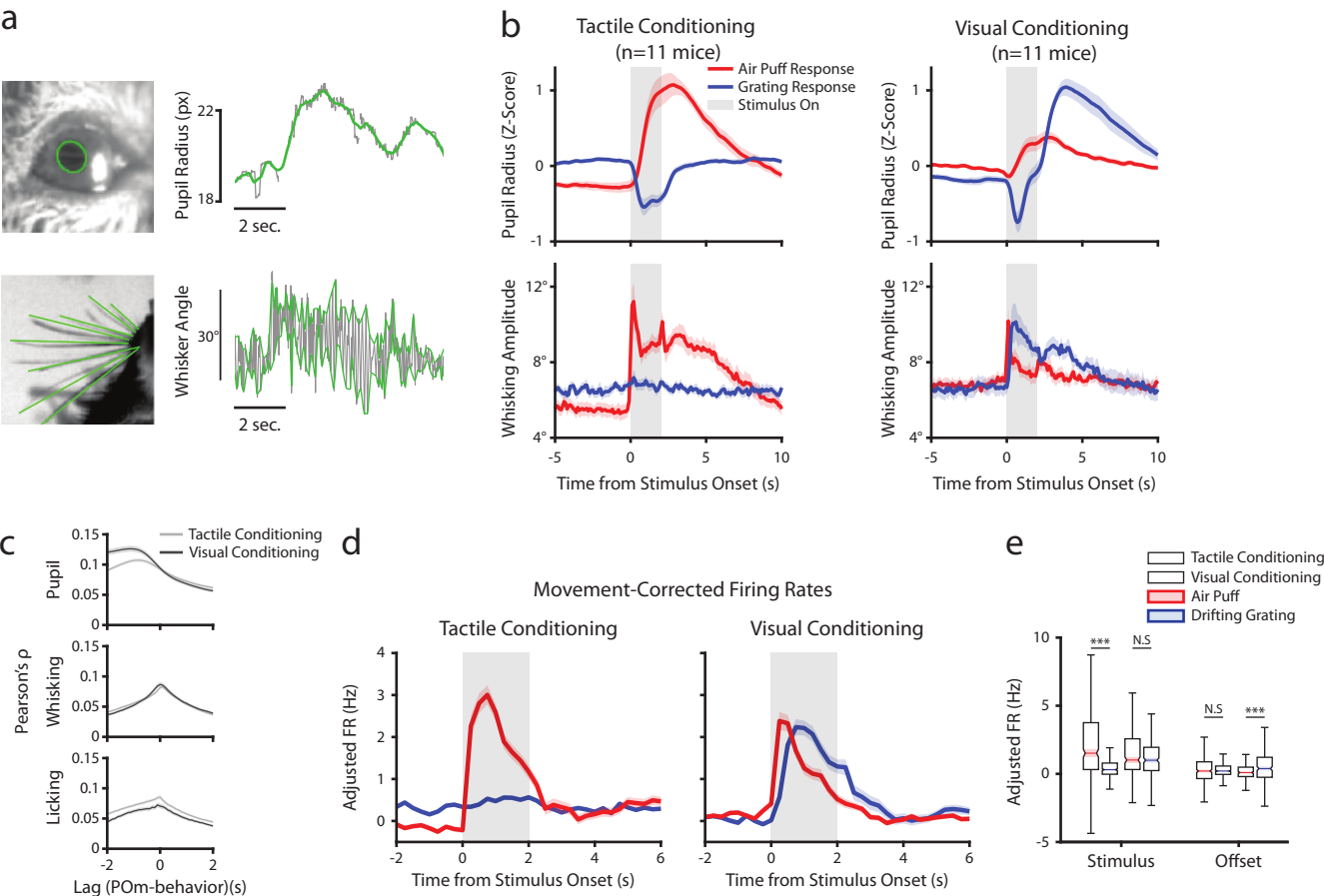

Figure 6: Conditioning also reshapes LP activity

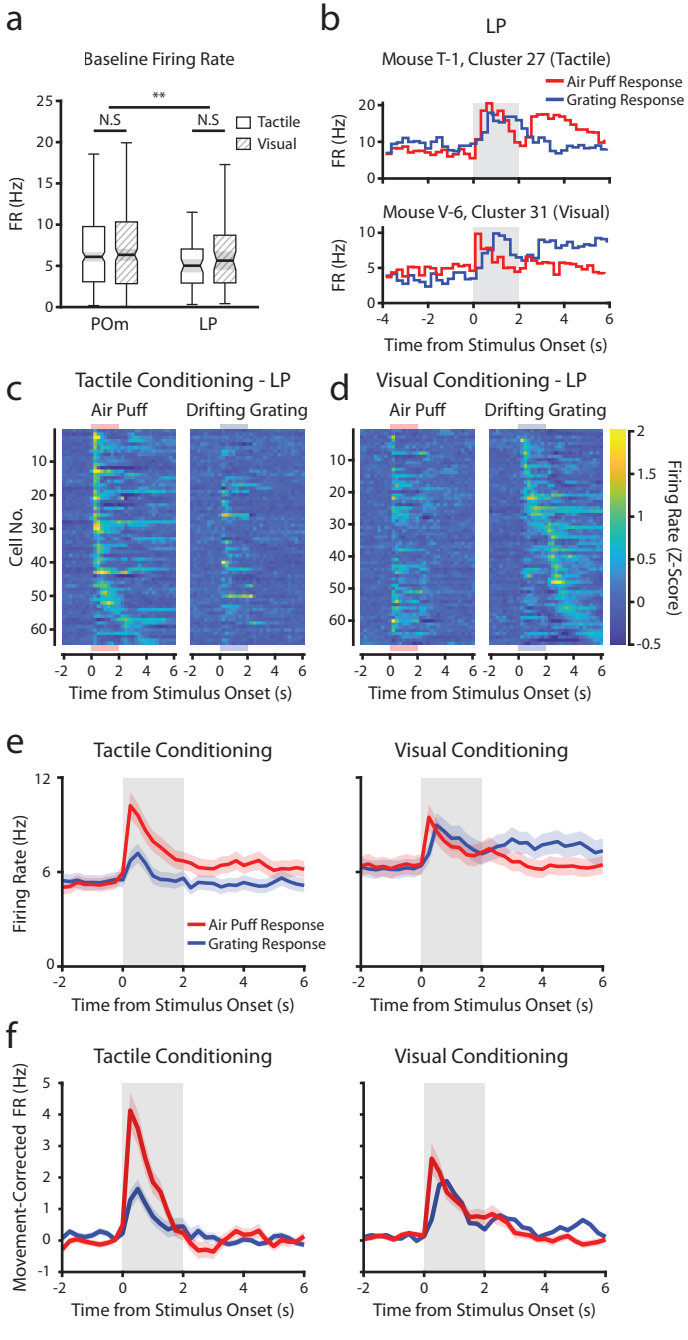

Figure S1: Manual curation of POm and LP cells.

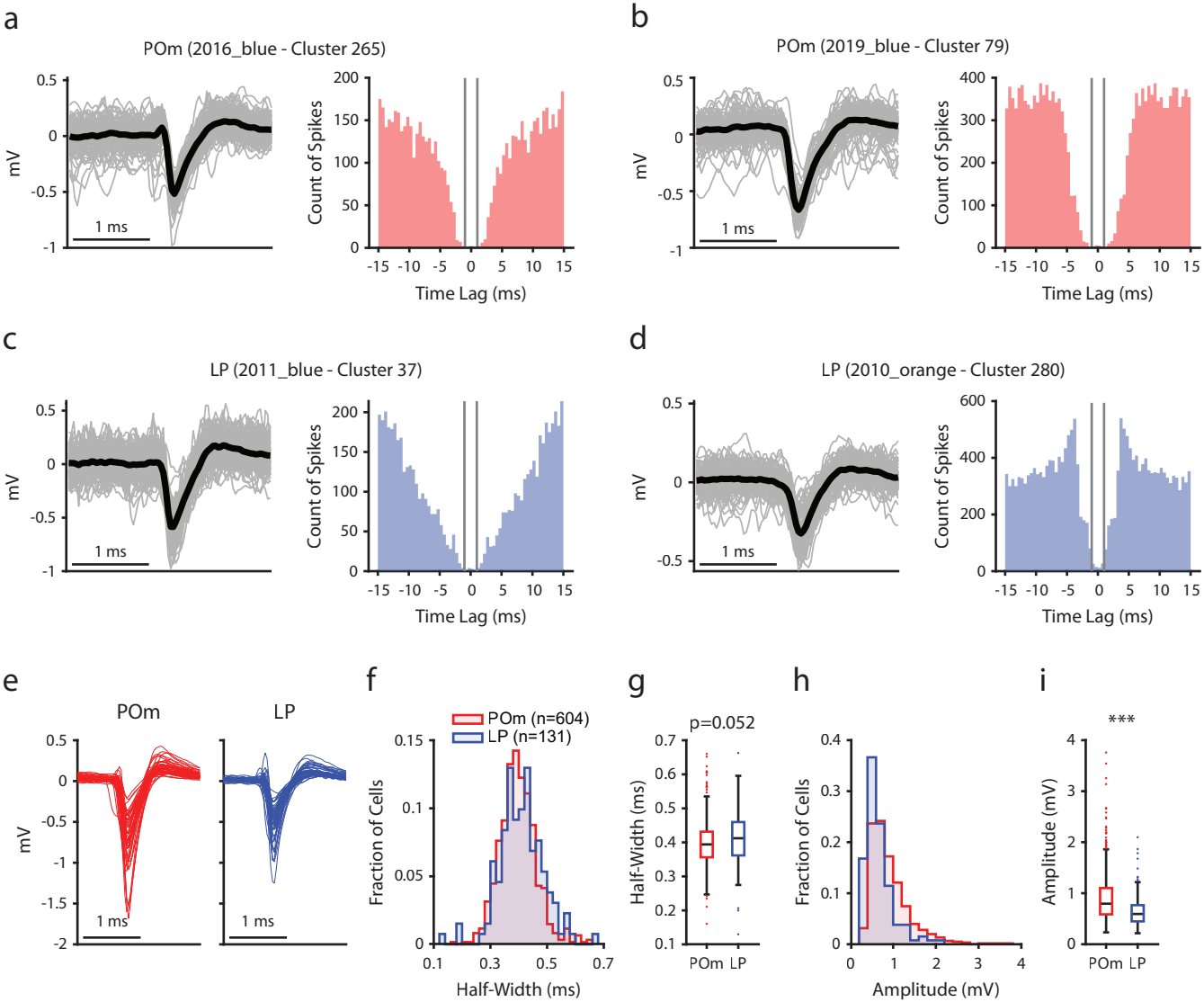

Figure S2: Conditioning alters sensory response latency in POm and LP

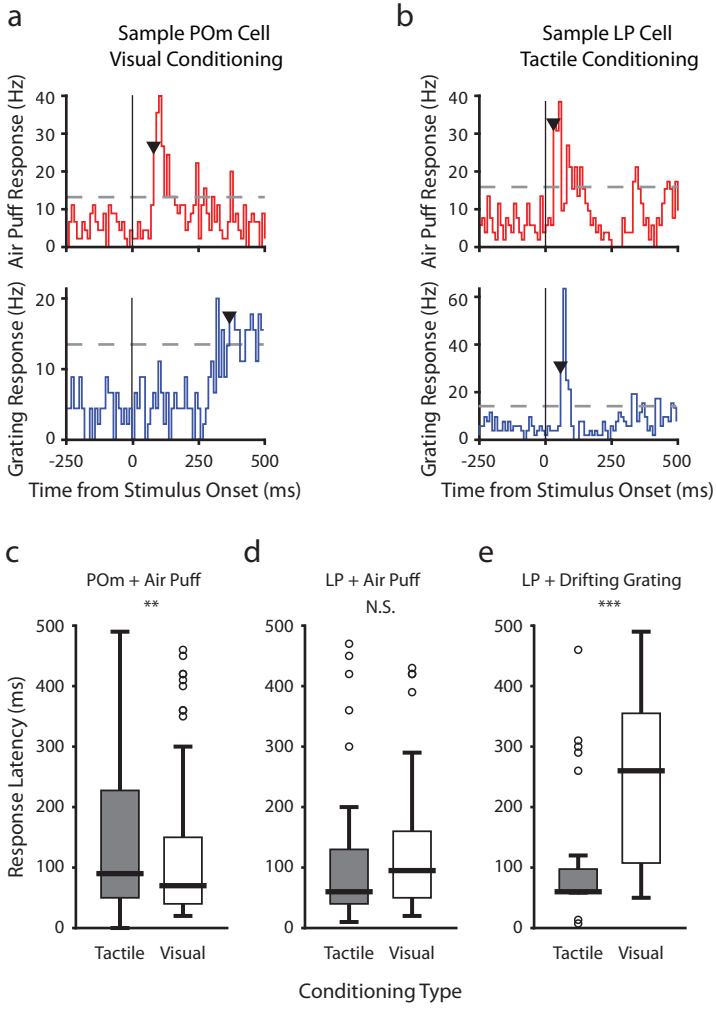
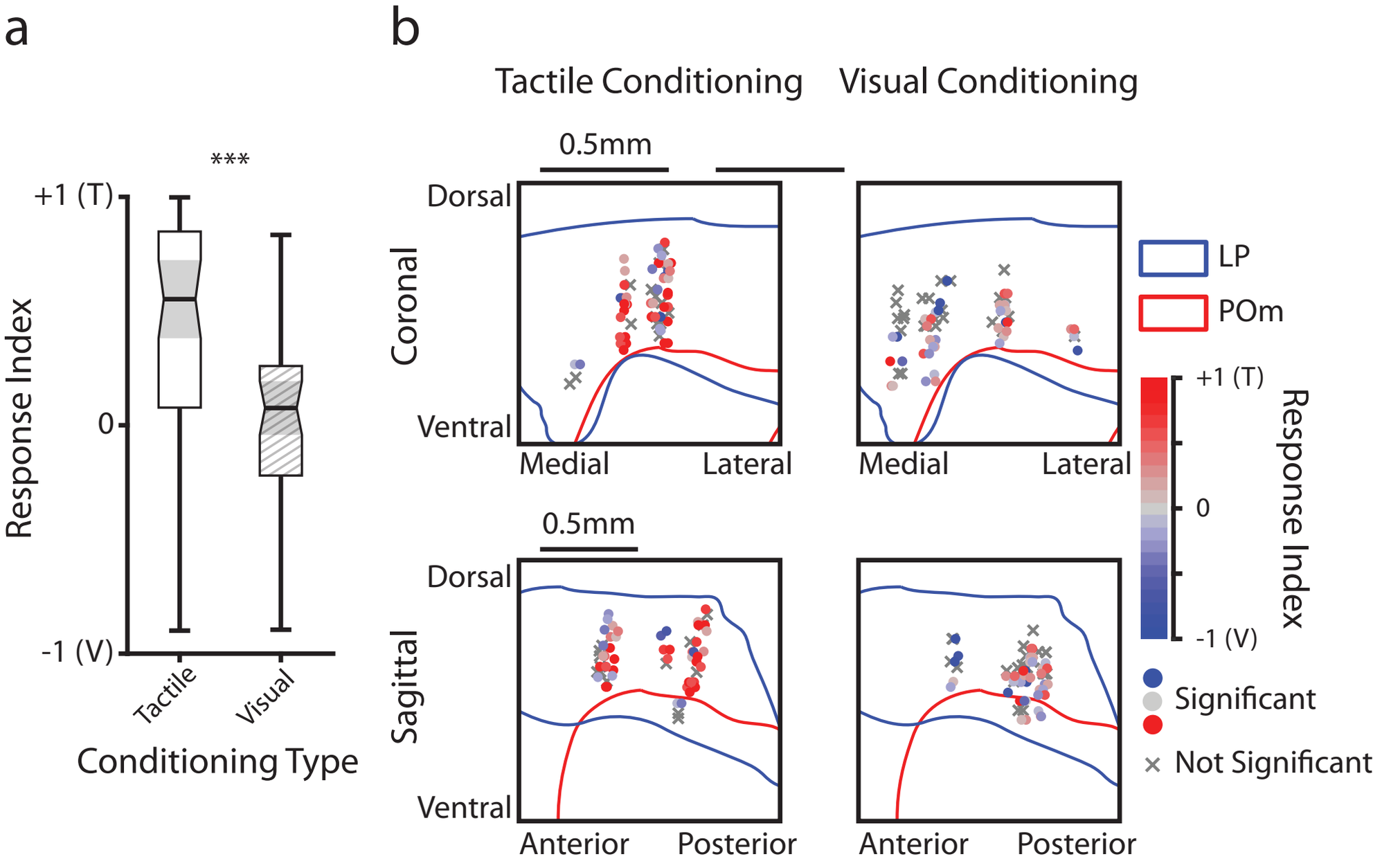
Figure S3: LP responses to tactile and visual stimuli as a function of anatomical location